Aromaticity

DOI: 10.1002/anie.201208289

Ruthenocenoporphyrinoids: Conformation Determines Macrocyclic π Conjugation Transmitted Across a d-Electron Metallocene**

Irena Grocka, Lechosław Latos-Grażyński, and Marcin Stępień*

Porphyrinoids provide an intriguing environment for advanced investigation of macrocyclic π aromaticity. Through extensive explorations including complementary efforts of experimental and theoretical chemists, it has been determined that π-electron conjugation in porphyrinoid analogues depends on the topology of the molecular framework, conformation of the macrocycle, tautomerism, and inner-core metal coordination.[1–5]

In a recent study the ferrocenothiaporphyrinoids **1** and **2**-H_2 (Scheme 1) showed the very first evidence for direct transmission of metallamacrocyclic π-electron conjugation

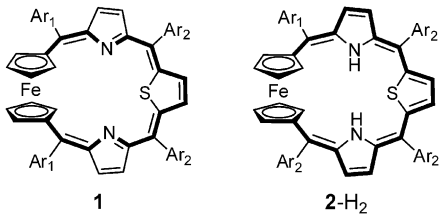

Scheme 1. The antiaromatic ferrrocenothiaporphyrin **1** and the aromatic dihydroferrocenothiaporphyrin **2**-H_2 (Ar_1 = Ph, Ar_2 = tol).

across a d-electron ferrocene, as experimentally documented by ^{1}H NMR spectroscopic data.[6] This observation remains in contrast with the magnetic properties of previously explored metallocenophanes, as none of classical ferrocenophanes[7] or ruthenocenonaphanes[8] containing the π-conjugated linker demonstrated features characteristic of macrocyclic aromaticity. At this stage the metallocene-conveyed aromatic behavior, the impact of the metal ion, and the rotational flexibility of metallocene unit remain to be explored.

Herein we report on the synthesis and characterization of ruthenocenoporphyrinoids whose magnetic properties correspond to macrocyclic antiaromaticity and aromaticity. These molecules provide an indication of direct transmission of π-electron conjugation across the d-electron ruthenocene sandwich. Significantly, the macrocyclic aromaticity is conformationally controlled by the mutual arrangement of the cyclopentadienyl (Cp) rings.

The ruthenocenothiaporphyrin **5** was obtained in a (3+1) macrocyclization reaction involving 1,1′-bis[phenyl(2-pyrrolyl)methyl]ruthenocene (**3**) and 2,5-bis[hydroxy(*p*-tolyl)-methyl]thiophene (**4**), which were condensed under Lindsey-type conditions (6% yield; Scheme 2).

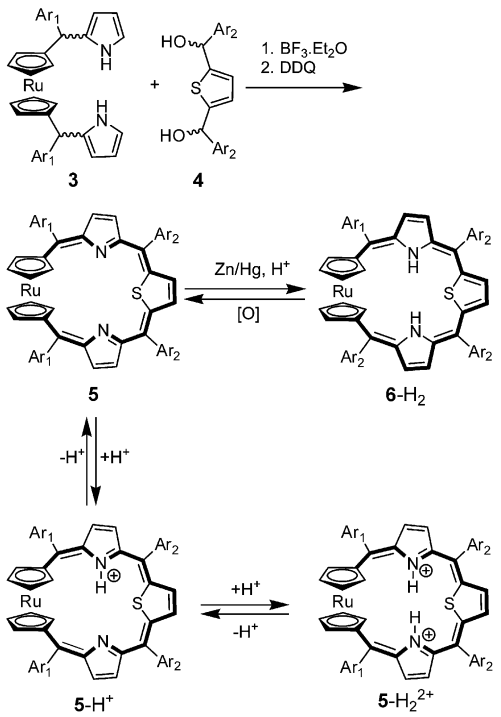

Scheme 2. Synthesis and reactivity of ruthenocenothiaporphyrin **5** (Ar_1 = Ph, Ar_2 = tol).

The molecular structure of **5** reveals that the π system is torsionally distorted, with the internal torsional angles of the 25,29-dicarba-27-thiapentapyrrin helix varying in the range from 5.2 to 13.2° (Figure 1). The two Cp rings adopt an anticlinal eclipsed conformation [the C_{Cp}-Ct-Ct′-$C_{Cp'}$ torsional angle ϕ equals 142.0°, Ct and Ct′ denote centroids of the respective Cp rings, C_{Cp} = C4, $C_{Cp'}$ = C21].

At 215 K, the ^{1}H NMR spectrum of **5** is consistent with the C_2 symmetry of the helical molecular framework (Figure 2b). Titration of **5** with trifluoroacetic acid (190 K, CD_2Cl_2) affords the well-defined monocation **5**-H^+ and subsequently the dication **5**-H_2^{2+}. The first protonation step lowers the observed spectral symmetry rendering all positions non-equivalent, but the addition of the second proton results in C_2

[*] I. Grocka, Prof. L. Latos-Grażyński, Dr. M. Stępień
Department of Chemistry, University of Wrocław
14 F. Joliot-Curie St., 50383 Wrocław (Poland)
E-mail: lechoslaw.latos-grazynski@chem.uni.wroc.pl
Homepage: http://llg.chem.uni.wroc.pl/

[**] Financial support from the Ministry of Science and Higher Education (Grant N N204 013536) and the National Science Centre (Grant 2012/04A/ST5/00593) are kindly acknowledged. DFT calculations were carried out at the Supercomputer Centers of Poznań and Wrocław.

Supporting information for this article is available on the WWW under http://dx.doi.org/10.1002/anie.201208289.

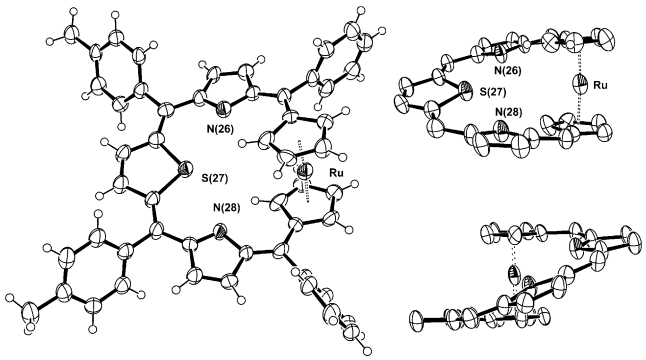

Figure 1. The molecular structure of **5** (left: perspective view; right: side views; aryl groups and hydrogen atoms omitted for clarity). The thermal ellipsoids represent 50% probability.

symmetry and yields a spectral pattern resembling that of **5**. The protonation can be readily reversed by addition of an amine base. Protonation affording **5**-H^+ and **5**-H_2^{2+} takes place at the pyrrolic nitrogen atoms, as documented by the appearance of the corresponding N(26)H resonance at $\delta =$ 16.43 ppm (**5**-H^+) and the N(26,28)H at $\delta = 18.04$ ppm (**5**-H_2^{2+}; see traces c and d in Figure S4 of the Supporting Information). The four ^{1}H NMR resonances of **5** corresponding to the ruthenocene-1,1′-diyl unit are found at $\delta = 10.76$ (H25,H29), 6.45 (H1,H24), 5.26 (H2,H23), and 3.34 (H3,H22) ppm and serve as the fingerprint of a peculiar electronic structure. The spread of ruthenocene chemical shifts increases due to protonation (**5**: $\delta = 7.42$ ppm; **5**-H^+; $\delta =$ 9.92 ppm; **5**-H_2^{2+}: $\delta = 10.08$ ppm). Such features, have not yet been detected for any ruthenocene derivatives including [4]ruthenocenophane, which contains a fully conjugated bridge and 1,1′-substituted ruthenocenyl rings in the synperiplanar conformation.[8]

Reduction of **5** with zinc amalgam was performed in [D_8]toluene under strictly anaerobic conditions to yield the dihydroruthenocenothiaporphyrin **6**-H_2. The macrocyclic diatropicity of this species is reflected by the chemical shift pattern (Figure 2a). Importantly, exposing the [D_8]toluene solution of **6**-H_2 to atmospheric dioxygen recovers **5** quantitatively in a matter of hours.

The synthetic work leading to the ruthenocenothiaporphyrin **7**-(*sp*)-H is summarized in Scheme 3.

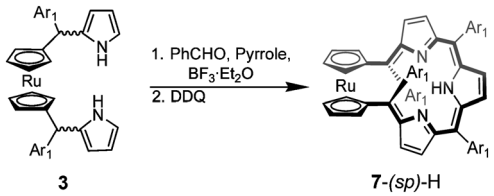

Scheme 3. Synthesis of ruthenocenoporphyrin **7**-(*sp*)-H ($Ar_1 =$ Ph).

The monoprotonated cation **7**-(*sp*)-H_2^+ acquires a peculiar conformation with $\phi = 13.1°$ (Figure 3) and the Cp rings, which are almost eclipsed, having an interplanar angle of 11° between them.[9] The π system of **7**-(*sp*)-H_2^+ is torsionally distorted, with the internal torsional angles of the 25,29-dicarba-27-pentapyrrin ligand varying in the range 10.0–25.5°. The linker reveals the bond-length pattern expected for aromatic carbaporphyrinoids with some bond equalizing

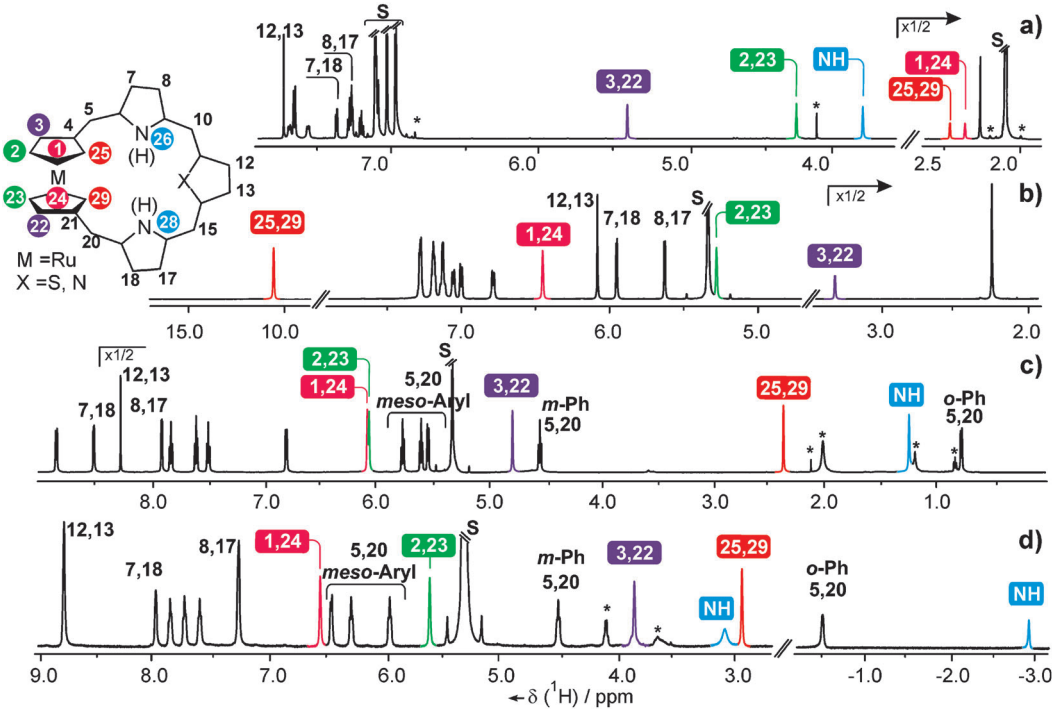

Figure 2. ^{1}H NMR spectra of the a) aromatic **6**-H_2 (250 K, [D_8]toluene), b) antiaromatic **5** (215 K, CD_2Cl_2), c) aromatic **7**-(*sp*)-H^{2+} (220 K, CD_2Cl_2), d) aromatic **7**-(*sp*)-H_3^{2+} (190 K, CD_2Cl_2). Resonance assignments shown only for diagnostic resonances.

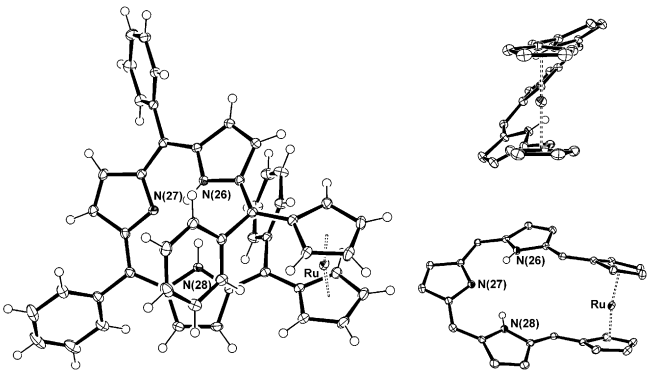

Figure 3. The molecular structure of **7**-(*sp*)-H_2^+ (left: front view; right: side views; aryl groups and hydrogen atoms omitted for clarity). The thermal ellipsoids represent 50% probability.

effect consistent with the observed aromaticity of this species.[1–3]

The ^{1}H NMR spectra of **7**-(*sp*)-H, **7**-(*sp*)-H_2^+, and **7**-(*sp*)-H_3^{2+} (Figures 2c,d; Figure S5 in the Supporting Information) are consistent with the C_2 symmetry of the helical molecular framework and the protonation of the nitrogen atoms for a given species [**7**-(*sp*)-H: N(27)H, **7**-(*sp*)-H_2^+: N(26)H, N(28)H, and **7**-(*sp*)-H_3^{2+}: N(26)H, N(27)H, N(28)H]. The macrocyclic diatropicity of these species is reflected by characteristic chemical shift patterns which are typical for aromatic meso-tetraarylporphyrins.[1,2] For instance the diagnostic β-hydrogen resonances of **7**-(*sp*)-H_2^+ are spread throughout the $\delta = 7.8$–8.5 ppm region (H7,H18: $\delta =$ 8.53 ppm, H8,H17: $\delta = 7.92$ ppm, and H12,H13: $\delta =$ 8.29 ppm) and the inner N(26)H and N(28)H protons move upfield to $\delta = 1.23$ ppm. The diatropic character of **7**-(*sp*)-H_2^+ is reflected by a smaller but consistent change of ruthenocene chemical shifts. The four ^{1}H NMR resonances corresponding to the ruthenocene-1,1′-diyl unit are found at $\delta = 2.35$ (H25,H29), 6.08 (H1,H24), 6.06 (H2,H23), and 4.78 (H3,H22) ppm. The *endo*-phenyl (at C5,C20) and *exo*-phenyl (at C10,C15) resonances reveal the substantial anisotropy of the shielding/deshielding macrocyclic effect (*endo*-Ph: *o*-Ph at $\delta = 0.76$ and 5.20 ppm; *m*-Ph at $\delta = 4.54$ ppm and $\delta = 5.76$ ppm, *p*-H at $\delta = 5.60$ ppm; *exo*-Ph: *o*-Ph at $\delta = 8.87$ and 6.81 ppm, *m*-Ph at $\delta = 7.83$ and 7.51 ppm, *p*-H at $\delta =$ 7.61 ppm).

In the case of porphyrin analogues, the ^{1}H NMR chemical shifts are a convenient experimental measure of aromatic character.[1–3,10] The ^{1}H NMR spectra of **5**, **5**-H^+, and **6**-H_2 demonstrate the peculiar differentiation of chemical shifts within the ruthenocene fragment (Figure 2). The range of ruthenocene chemical shifts observed for **5** ($\delta = 10$–3 ppm), **5**-H^+ ($\delta = 13$–3 ppm), and **5**-H_2^{2+} ($\delta = 14$–3 ppm) are consistent with a macrocyclic paratropic ring current creating considerable magnetic anisotropy. This paratropic current influences the shifts of pyrrole and thiophene β-hydrogen atoms, which experience upfield shifts (relative to the nonaromatic reference molecules).[11] Significantly, in the dihydro derivative **6**-H_2, the sign of the anisotropy is reversed and is consistent with the presence of a diatropic current in the macrocycle. This switching of the ring current sign upon a formal two-electron reduction/oxidation is a typical feature of π-electron aromatics. In the present case, however, the macrocyclic conjugation in **5** and **6**-H_2 must necessarily involve the ruthenium atom of ruthenocene unit, which principally participates in bonding through its d orbitals. Indeed ruthenocenothiaporphyrin reproduces the fundamental spectroscopic features reported for appropriate ferrocenothiaporphyrins **1** and **2**-H_2.[6] Ferroceno- and ruthenocenothiaporphyrins (**1**, **2**-H_2, **5**, **6**-H_2) acquire similar convex macrocyclic conformations enforced by the anticlinal (eclipsed) arrangement of metallocyclopendienyl moieties. Consequently both d electron metallocenes (ferrocene or ruthenocene) contribute to a macrocyclic π-electron conjugation pathway in an analogous manner.

In the context of the metallocene role in the macrocylic delocalization, the most remarkable effect has been observed for the ruthenocenoporphyrin **7**-H and its mono- and diprotonated cations. The hingelike flexibility of the 1,1′-disubstitued ruthenocene unit provides a unique way to determine the overall macrocyclic conformation, thus engaging an additional three-dimensional factor (Figure 4). Thus **7**-(*sp*)-H, **7**-(*sc*)-H, and **7**-(*ac*)-H conformers refer directly to synperiplanar, synclinal (eclipsed), and anticlinal (eclipsed) conformations, respectively, for the built-in ruthenocene.

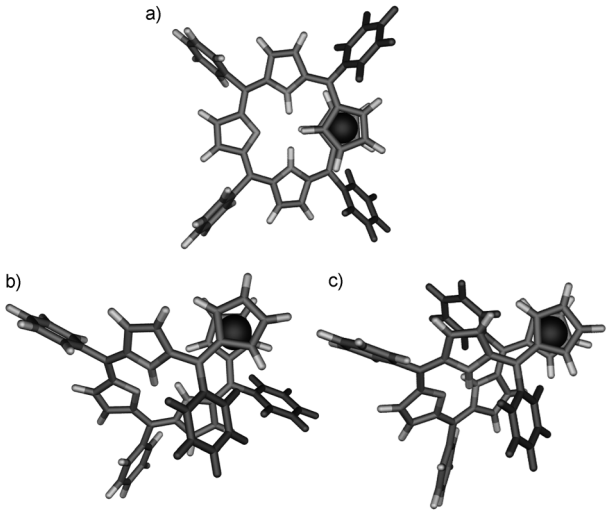

Figure 4. DFT optimized structures of a) **7**-(*ac*)-H_2^+, b) **7**-(*sc*)-H_2^+, and c) **7**-(*sp*)-H_2^+.

In the series of porphyrins and its 21 heteroanalogues (O, S, Te, P), the ^{1}H NMR aromatic spectroscopic properties related to macrocyclic aromaticity provide the well-defined fingerprint of electronic structures.[1,3,12] Accordingly, we have presumed that the hypothetical **7**-(*ac*)-H porphyrinoid (Figure 4) and its thia-analogue **5**, described herein, will produce similar patterns of resonances, thus reflecting their antiaromaticity. In contrast to **5**, the ruthenocenoporphyrin **7**-(*sp*)-H and its cations demonstrate the characteristic signs of macrocyclic diatropicity. Here we point out that structural/conformational effects are instrumental for the control of magnetic properties as reflected by the aromatic versus antiaromatic switch, thus preserving the constant number

π electrons in the bridging unit. In terms of π conjugation, the in-phase overlaps of the adjacent p orbitals of the dicarbapentapyrrin (characteristic for **7**-(*ac*)-H_2^+) will be preserved in **7**-(*sc*)-H_2^+ and **7**-(*ac*)-H_2^+. Clearly, the present work reveals a novel facet of porphyrinoid aromaticity proving that the macrocyclic π conjugation transmitted across a d-electron metallocene is conformationally controlled.

The major obstacle to applying the annulene model to **5, 6**-H_2, or **7**-H is that in each case the conjugation pathway passes through the ruthenocene subunit, which does not easily lend itself to the valence bond theoretical description.[13,14] As a matter of fact, the analogous complications have been already encountered in analysis of electron delocalization for metallabenzenes, metallacycloheptatrienes, and metallacyclooctatetraenes.[15–17] The helical structures of metallocenoporphyrinoids preserve the in-phase overlap of p orbitals at the carbon backbone, thus eventually affording a Hückel or Möbius-type topology of the resulting molecular orbital which is actually determined by appropriate in-phase or out-of-phase overlap with the orthogonal d_{xz} and d_{yz} orbitals of the metallocene. These d orbitals are oriented either perpendicular or parallel to the porphyrinoid perimeter. In fact, the first overlap mode seems to be dominant for synclinal and the second one for antiperiplanar conformers of ruthenocene. Thus for the given number of engaged electrons, a metallocenoporphyrinoid will reveal an aromatic or antiaromatic behavior, which is controlled by the orientation of the d orbitals involved. In the intermediary situation ($0° < \phi < 180°$) both scenarios are simultaneously contributing.

To gain further insight into the electronic structure, DFT calculations were performed for the meso-substituted species **7**-(*sp*)-H_2^+, **7**-(*sc*)-H_2^+, and **7**-(*ac*)-H_2^+, (Figure 4). The relative energies increase in a series: **7**-(*sp*)-H_2^+ (0 kcal mol^{-1}), **7**-(*ac*)-H_2^+ (7.69 kcal mol^{-1}), and **7**-(*sc*)-H_2^+ (8.11 kcal mol^{-1}). Comparison of the geometries optimized for **7**-(*sp*)-H_2^+, **7**-(*sc*)-H_2^+, and **7**-(*ac*)-H_2^+ at the B3LYP/LANL2DZ level of theory reveals that the effect of macrocyclic π conjugation on the bond lengths is rather subtle. Specifically, the C4-C_{meso} and C21-C_{meso} distances vary slightly [**7**-(*sp*)-H_2^+ 1.438, **7**-(*sc*)-H_2^+ 1.451 and 1.441 and **7**-(*ac*)-H_2^+, 1.467 Å]. Analyses of the bond lengths in the tripyrrin section of **7**-(*sp*)-H_2^+, **7**-(*sc*)-H_2^+, and **7**-(*ac*)-H_2^+ show that a weak bond equalizing effect is indeed present in **7**-(*sp*)-H_2^+, and is consistent with the observed aromaticity of this species. This effect, however, is not strong enough to provide sufficient evidence for the aromaticity of **7**-(*sp*)-H_2^+.

^{1}H NMR chemical shifts observed for **7**-(*sp*)-H_2^+, including the unusual diatropic ring current, can be reproduced using the GIAO-DFT method at the B3LYP/LANL2DZ level of theory (Table S4, Figure S22), in line with our earlier computational work.[6] Subsequently, the analysis was extended to the analogously determined chemical shift patterns of hypothetical **7**-(*sc*)-H_2^+ and **7**-(*ac*)-H_2^+ (see Table S4 in the Supporting Information). The impact of conformation on the chemical shift patterns for the diagnostically essential resonances is illustrated in Figure 5. Comparison of these patterns demonstrate spectacular distinctions between ruthenocenoporphyrinoids conjugated in different manners. In the case of **7**-(*sp*)-H_2^+ and **7**-(*sc*)-H_2^+, diatropic contributions to the chemical shift are dominant, whereas the paratropic contribution is essential for **7**-(*ac*)-H_2^+.

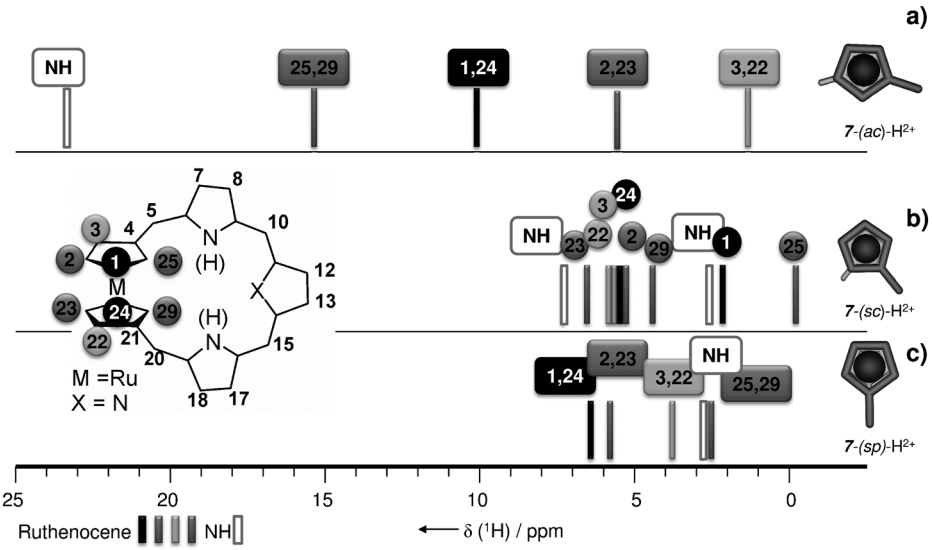

Figure 5. Schematic representation of the calculated ^{1}H NMR spectra for a) **7**-(*ac*)-H_2^+, b) **7**-(*sc*)-H_2^+, and c) **7**-(*sp*)-H_2^+. The conformation of ruthenocene shown to the right of each spectrum.

Ruthenocenoporphyrinods are shown, for the very first time, to have a π-conjugated surface which adopts topologically distinct states because of rotational motions involving a metallocene hinge. This property is reflected by the macrocyclic aromaticity and antiaromaticity for the identical number of π electrons. Additional research is aimed at macrocyclic systems which are flexible enough to accommodate different metallocenoporphyrinoid conformers in a single macrocyclic structure, thus allowing control of the stepwise conformational processes by applying external stimuli.

Received: October 15, 2012
Published online: November 28, 2012

Keywords: aromaticity · NMR spectroscopy · porphyrinoids · ruthenium · structure elucidation

[1] M. Pawlicki, L. Latos-Grażyński in *Handbook of Porphyrin Science: with Applications to Chemistry, Physics, Materials Science Engineering, Biology and Medicine*, *Vol. 2* (Eds.: K. M. Kadish, K. M. Smith, R. Guilard), World Scientific Publishing, Singapore, **2010**, pp. 104 – 192.
[2] M. Stępień, L. Latos-Grażyński in *Aromaticity in Heterocyclic Compounds*, *Vol. 19* (Ed.: T. M. Krygowski), Springer, Berlin, **2009**, pp. 83 – 154.
[3] M. Stępień, N. Sprutta, L. Latos-Grażyński, *Angew. Chem.* **2011**, *123*, 4376 – 4430; *Angew. Chem. Int. Ed.* **2011**, *50*, 4288 – 4340.
[4] M. Toganoh, H. Furuta, *Chem. Commun.* **2012**, *48*, 937 – 954.
[5] S. Saito, A. Osuka, *Angew. Chem.* **2011**, *123*, 4432 – 4464; *Angew. Chem. Int. Ed.* **2011**, *50*, 4342 – 4373.
[6] I. Simkowa, L. Latos-Grażyński, M. Stępień, *Angew. Chem.* **2010**, *122*, 7831 – 7835; *Angew. Chem. Int. Ed.* **2010**, *49*, 7665 – 7669.
[7] R. W. Heo, T. R. Lee, *J. Organomet. Chem.* **1999**, *578*, 31 – 42.
[8] J. K. Pudelski, M. R. Callstrom, *Organometallics* **1994**, *13*, 3095 – 3109.
[9] CCDC 903282 (**5**) and 903276 ([**7**-(*sp*)-H_2](CF_3COO-$CF_3COOH)_2$]) contain the supplementary crystallographic data for this paper. These data can be obtained free of charge from The Cambridge Crystallographic Data Centre via www.ccdc.cam.ac.uk/data_request/cif.
[10] M. Stępień, L. Latos-Grażyński, L. Szterenberg, *J. Org. Chem.* **2007**, *72*, 2259 – 2270.
[11] M. Stępień, I. Simkowa, L. Latos-Grażyński, *Eur. J. Org. Chem.* **2008**, 2601 – 2611.
[12] L. Latos-Grażyński in *The Porphyrin Handbook*, *Vol. 2* (Eds.: K. M. Kadish, K. M. Smith, R. Guilard), Academic Press, New York, **2000**, pp. 361 – 416.
[13] L. Pauling, *The Nature of the Chemical Bond*, Cornell University Press, Ithaca, NY, **1960**.
[14] F. Weinhold, C. R. Landis, *Valency and Bonding: A Natural Bond Orbital Donor-Acceptor Perspective*, Cambridge University Press, Cambridge, **2005**.
[15] D. L. Thorn, R. Hoffman, *New J. Chem.* **1979**, *3*, 39 – 45.
[16] J. R. Bleeke, *Chem. Rev.* **2001**, *101*, 1205 – 1227.
[17] M. Mauksch, S. B. Tsogogoeva, *Chem. Eur. J.* **2010**, *16*, 7843 – 7851.

